Precambrian Research 237 (2013) 101–115

Contents lists available at ScienceDirect

Precambrian Research

journal homepage: www.elsevier.com/locate/precamres

Eastward transport of the Monapo Klippe, Mozambique determined from field kinematics and computed tomography and implications for late tectonics in central Gondwana

Jodie A. Miller[a,*], Carly Faber[a], Christie D. Rowe[b,c], Paul H. Macey[d], Anton du Plessis[e]

[a] Department of Earth Sciences, Stellenbosch University, Private Bag X1, Matieland 7602, South Africa
[b] Department of Earth and Planetary Sciences, McGill University, 3450 University Street, Montréal, QC H3A 0E8, Canada
[c] University of Cape Town Department of Geological Sciences, Private Bag X3, Rondebosch 7701, South Africa
[d] Western Cape Unit, Council for Geoscience, PO Box 572, Bellville 7530, South Africa
[e] Computed Tomography Unit, Central Analytical Facility, Stellenbosch University, Private Bag X1, Matieland 7602, South Africa

ARTICLE INFO

Article history:
Received 19 April 2013
Received in revised form 29 August 2013
Accepted 6 September 2013
Available online xxx

Keywords:
Monapo Klippe
Kinematic indicators
Computed tomography
East African Orogen
Gondwana assembly

ABSTRACT

We present a detailed kinematic study of the boundary between the Monapo Klippe and the underlying Nampula Block in northern Mozambique. The Monapo Klippe is an allochthonous klippe of granulite-facies metamorphic rocks with subsidiary granitic and mafic intrusive rocks. The klippe overlies the Nampula Block which is made up of ortho- and paragneisses that are lower metamorphic grade and considerably older than the rocks of the Monapo Klippe. The boundary between the klippe and the underlying Nampula Block is a distinct mylonitic shear zone of variable width. The mylonite composition varies with the local footwall lithology but the dominant composition is quartz-rich with minor feldspar augen and biotite. The mylonite is interpreted to have formed as an early broad ductile shear zone that evolved during multiple phases of shearing to a narrow high-strain, lower temperature mylonite horizon. Kinematic indicators observed in outcrop, thin section, and image slices from X-ray computed tomography of three-dimensional mylonitic fabrics record top-to-east motion. The granulite-facies Cabo Delgado Nappe Complex, which lies to the north of the Monapo Klippe, has been hypothesized as the root terrane for the klippe. The Cabo Delgado Nappe Complex records top to the north-west motion at around 630–610 Ma. However, granitic and pegmatitic rocks that intrude the Monapo Klippe, and which also cross-cut the mylonite fabric as well as being deformed by it, are considered to be part of the Cambrian Murrupula Suite dated at between 530 and 470 Ma. This suggests that the emplacement of the Monapo Klippe over the Nampula Block is part of a later extensional phase post 530 Ma associated with east-directed post-orogenic collapse following Gondwana assembly.

1. Introduction

During the amalgamation of Gondwana, between ~630 and 480 Ma, numerous crustal blocks collided to form a number of major orogenic belts along the eastern edge of Africa (Meert, 2003; Stern, 2004; Collins and Pisarevsky, 2005). The timing and orientation of collision of these different crustal blocks have been the subject of ongoing debate within this part of Gondwana (Pinna, 1995; Sacchi et al., 2000; Viola et al., 2008; Jacobs et al., 2008; Grantham et al., 2008, 2013; Ueda et al., 2012a; Macey et al., 2013) and elsewhere within the supercontinent (Kriegsman, 1995; Shackelton, 1996; Jacobs et al., 1998; Fitzsimons, 2000; Collins et al., 2007; Kelsey et al., 2008; Grantham et al., 2008; Baba et al., 2010; Tucker et al., 2011; Collins et al., 2013). The ongoing debate is driven by three main problems: (1) the paucity of outcrop in key areas where orogens are thought to cross or intersect, (2) resolution the timing of orogeny and its duration in different parts of the Gondwana supercontinent; and (3) determination of the transport direction of what are in most cases reworked high-grade metamorphic rocks. Work to address problems (1) and (2) is ongoing and continuous. For example, recently there has been a major research focus on resolving the geological history of the Sør Rondane Mountains in Antarctica, considered to be one of several keystones for understanding assembly of central Gondwana. Outcrop is very scarce and hard to access but the recent work has made significant inroads into understanding the timing relationships of major geological events in this region (Satish-Kumar et al., 2013 and references therein). Nevertheless, attempts to address problem (3) remain problematic principally because of the lack of reliable and widespread kinematic indicators that can be linked to

* Corresponding author. Tel.: +27 218083121; fax: +27 218083129.
E-mail address: jmiller@sun.ac.za (J.A. Miller).

0301-9268/$ – see front matter © 2013 Elsevier B.V. All rights reserved.
http://dx.doi.org/10.1016/j.precamres.2013.09.007

specific parts of an orogenic cycle. Although there has recently been a more concerted effort to clarify the transport vectors for different components of the African Gondwana components (e.g. Viola et al., 2008; Thomas et al., 2012; Ueda et al., 2012a), such studies are still generally rare.

The Monapo Klippe in northern Mozambique, another keystone for understanding assembly of central Gondwana, illustrates how the identification of transport kinematics is critical to understanding terrane amalgamation. The klippe is an exotic block of granulite-facies ortho- and paragneisses that has been intruded by granitic and ultramafic rocks. It currently sits on top of Mesoproterozoic rocks of the Nampula Block and is separated from them by a distinct mylonite zone, called the marginal mylonite (Macey et al., 2013). Dating of the granulite-facies metamorphism and granitic intrusions within the klippe has shown that intrusion and metamorphism were synchronous at ~635 Ma (Macey et al., 2013). Since the lower grade Nampula gneisses do not record this metamorphic event (Macey et al., 2010; Grantham et al., 2013), the klippe must have been emplaced over the Nampula Block after 635 Ma. However, juxtaposition of the Monapo Klippe over the Nampula Block probably occurred before ~525–480 Ma when both the klippe and the Nampula gneisses were metamorphosed at high temperature and low pressure conditions associated with emplacement of Cambrian to Ordovician granites of the Murrupula Suite (Macey et al., 2010, 2013; Ueda et al., 2012b). The sense of shear in the marginal mylonite and the exact timing of transport are thus pivotal to resolving the transportation history of the Monapo Klippe and the nature of its emplacement over the Nampula block.

The marginal mylonite has a strong foliation consistent with very high shear strain and/or considerable syn-shear flattening, but static recrystallization has overprinted the fine groundmass which now has an equigranular texture. Kinematic indicators such as clast asymmetry are difficult to conclusively interpret in outcrop and thin-section due to the high degree of flattening. In this contribution, we attempt to clarify the transport history of the Monapo Klippe by using a combination of traditional field geology, microstructural studies and X-ray computed tomography (XCT) of the mylonite samples. This multi-faceted and multi-scale approach provides the best available constraints on the direction of klippe transport and places the geological history of the Monapo Klippe more accurately within the context of central Gondwana assembly. Finally we hypothesize on what the likely direction of regional collision was during exhumation at the end of the Neoproterozoic to Ordovician assembly of the Gondwana supercontinent.

2. Regional geology

In northeast Mozambique, the Lúrio Belt is a major WSW–ENE trending, NNW-dipping tectonic zone separating two major continental blocks (Fig. 1). To the south of the Lúrio Belt are predominantly amphibolite-facies felsic orthogneisses and subsidiary paragneisses with Mesoproterozoic (~1150–1075 Ma) protolith ages. The five main rock suites (Mocuba Complex, Rapale Gneiss, Mamala Gneiss, Molòqué Complex and Culicui Suite) are collectively referred to as the Nampula Block (Macey et al., 2010; Ueda et al., 2012a) and record an early metamorphism between 1110 and 1080 Ma overprinted by amphibolite-facies metamorphism between 540 and 490 Ma (Bingen et al., 2009; Macey et al., 2010; Ueda et al., 2012a). To the north of the Lúrio Belt are amphibolite-facies felsic orthogneisses (Unango and Marrupa Complexes) with slightly younger Mesoproterozoic to Neoproterozoic (~1060–945 Ma) protolith ages. These complexes, along with other granulitic rocks further east, are collectively referred to as the Namuno Block (Grantham et al., 2008). This block also records an early metamorphism, albeit younger (~900 Ma) than that in the Nampula Block. However, the dominant metamorphic overprint occurred at 555 Ma in the Marrupa Complex and between ~570 and ~530 Ma in the Unango Complex (Bingen et al., 2009; Ueda et al., 2012b), slightly older than that recorded in the Nampula Block (Macey et al., 2010). These differences in age, along with the

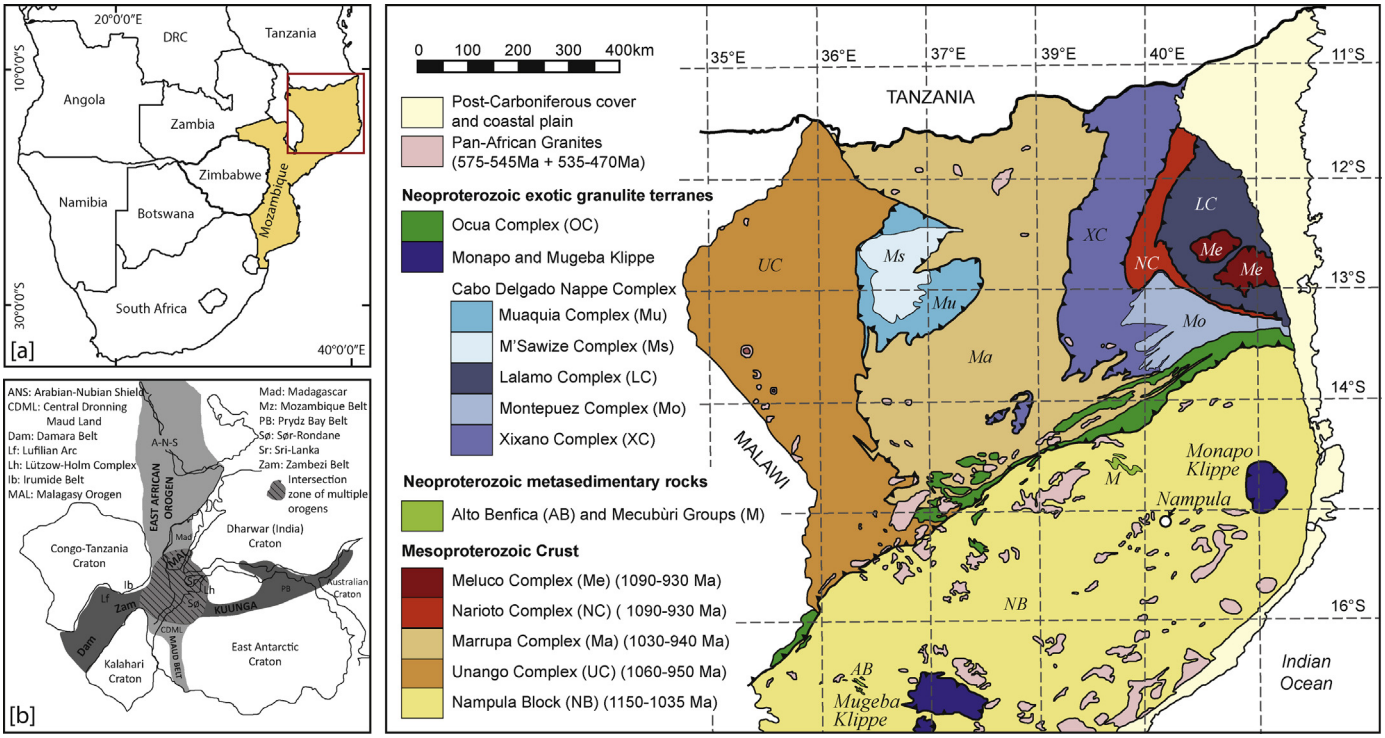

Fig. 1. Simplified geological map of north east Mozambique after Norconsult Consortium (2007a,b), Macey et al. (2007) and Grantham et al. (2007) showing the main lithostratigraphic units. Top inset [a] shows location of study area within southern Africa. Bottom inset [b] shows reconstruction of Gondwana during the Cambrian after Meert (2003), with the locations of the East African Orogen, Kuunga Orogen and Malagasy Orogen shown.

intensely tectonized character and strong linear aeromagnetic signature of the Lúrio Belt have led numerous authors to propose that the Lúrio Belt represents a major Gondwana suture zone (Grantham et al., 2008, 2013; Bingen et al., 2009; Macey et al., 2010).

Tectonically overlying the Nampula Block, Marrupa and Unango Complexes are a series of granulitic terranes that are interpreted to be remnants of a continental-scale Neoproterozoic upper nappe sheet (Viola et al., 2008; Grantham et al., 2008; Macey et al., 2013). To the north of the Lúrio Belt, this nappe sheet is represented by the Cabo Delgado Nappe Complex (Viola et al., 2008), a series of granulite-facies thrust slices imbricated over the Marrupa and Unango complexes prior to 555 Ma (Bingen et al., 2009). Viola et al. (2008) interpreted these thrust slices to be northwest vergent. To the south of the Lúrio Belt, the Monapo Klippe is an allochthon of similar material overlying the Nampula Block and separated from it by a mylonite zone (Macey et al., 2013). The klippe is dominated by strongly deformed granulite-facies rocks of variable composition belonging to the Metachéria Metamorphic Complex. Granulite-facies metamorphism has been dated at 635 Ma (Macey et al., 2013). Two intrusive suites are present in the klippe, the quartz-bearing Ramiane Suite granites, which are variably deformed to undeformed, and the foid-bearing ultramafic Mazerapane Suite gabbros and nepheline-syenites which are relatively undeformed. The Ramiane Suite appears to have intruded synchronously with granulite-facies metamorphism at 637 Ma, but underwent a later metamorphic event at 596 Ma (Macey et al., 2013). The Mazerapane Suite is currently undated. On the basis of the above information, the Monapo Klippe is demonstrably different in geological character to the underlying Nampula Block gneisses and this has formed the basis for its interpretation as a klippe. Similar conclusions have been made regarding the Mugeba Klippe which also lies to the south of the Lúrio Belt (Fig. 1) (Pinna et al., 1993; Kröner et al., 1997).

In addition to the allochtonous Monapo and Mugeba klippen, the Nampula Block is unconformably overlain by Neoproterozoic meta-sedimentary rocks (conglomerates, arenites and pelites) of the Mecubúri and Alto Benfica Groups (Thomas et al., 2010; Fig. 1). Dating of detrital zircons from the Mecubúri Group indicates that the source rocks are derived from the Namuno Block and not the Nampula Block and that the maximum depositional age is 530 Ma implying that the Namuno and Nampula terranes were adjoined by this time. Subsequent to the deposition of these meta-sedimentary rocks, the Nampula Block was intruded by weakly to undeformed post-orogenic Cambrian granites of the Murrupula Suite between ~530 and 480 Ma (Bingen et al., 2009; Grantham et al., 2007; Macey et al., 2007; Ueda et al., 2012a). However, these granites do not appear to have intruded into the Monapo Klippe, although pegmatites that may be related to the Murrupula Suite intrude into the marginal mylonite. Ueda et al. (2012a) interpret these granites as the result of post-orogenic collapse of the East African Orogen and high heat flow associated with lithospheric delamination, whereas Grantham et al. (2013) interpret them as a result of crustal overthickening during continental collision associated with the slightly younger E–W trending Kuunga Orogeny of Meert (2003) (Fig. 1).

3. The marginal mylonite zone

The Monapo Klippe is everywhere underlain by a zone of mylonite called the marginal mylonite (Macey et al., 2013). Although this zone is inferred to be continuous on the basis of geophysical and Landsat imagery, outcrop exposure of the mylonite is extremely poor. The topographic relief of the klippe is low with respect to the surrounding Nampula gneisses and the soil cover is extensive. Macey et al. (2013) delineated the marginal mylonite on the basis of principal component analysis performed on Landsat 7 ETM+ imagery as well as known field relationships. The extent of the mylonite zone determined in this way is shown in Fig. 2. The prominent bulge present on the south west margin of the klippe in Grantham et al. (2008, 2013) and BULGARGEOMIN (1984) was interpreted by Macey et al. (2013) to represent thrust slices within the footwall that are being emphasized by topography and therefore not actually part of the Monapo Klippe or the marginal mylonite. This was confirmed by field observations along a transect of the Monapo River from the town of Monapo into the Monapo Klippe, where an extensive footwall damage zone was encountered (see below Location D).

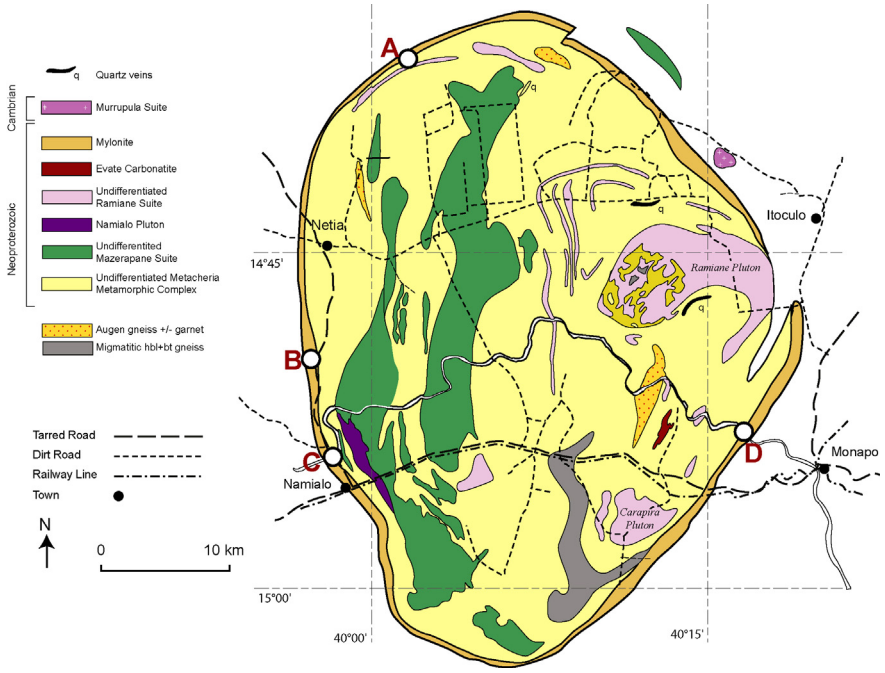

Fig. 2. Simplified geological map of the Monapo Klippe after Macey et al. (2013) showing the main lithostratigraphic units and the position of the marginal mylonite. Footwall geology is not indicated but is broadly TTG gneisses of the Nampula Block.

The exact thickness of the marginal mylonite has been difficult to determine because in only one location has the full thickness of the mylonite been observed. In all other locations, the boundaries of the mylonite are obscured by soil cover. Where the mylonite has been observed it is only a few meters thick with a pervasive planar shear fabric. Upper bounds on the thickness of the mylonite can be estimated from the remote sensing and suggest that the mylonite rarely exceeds 70 m. Compositionally, the marginal mylonite is very heterogeneous as a result of different rock types being incorporated into the mylonite zone. The dominant composition is a quartz-rich mylonite (Fig. 3a), derived from the abundant intermediate quartzo-feldspathic gneisses in the Metacheria Metamorphic Complex and/or the granitic to tonalitic footwall gneisses. Other compositions encountered included amphibole + quartz, probably derived from the more mafic lithologies (Fig. 3b), as well as granitic mylonites, probably derived from rocks of the Ramiane Suite. The mylonite has undergone extensive static recrystallization and annealing such that the quartz-feldspar matrix is uniformly fine-grained (1–3 mm) and equigranular and no shear microstructures remain. However, at a mesoscopic scale scarce rotated augen and clastic grains within the mylonitic fabric, and rare planar fabrics have the potential to indicate shear sense. Grains with extended tails are often highly symmetrical (ϕ-clasts), suggesting a high degree of shear strain and flattening, with asymmetrical σ- and δ-clasts being considerably rarer.

A ductile shear fabric in the footwall generally increases in intensity toward the marginal mylonite. This sheared damage zone cross cuts the granitic gneisses of the Culicui Suite and interleaved supracrustal gneisses of the Mamala and Molócuè Groups which collectively form the immediate footwall to the Monapo Klippe. Fabric intensity observed along a 7.5-km transect from the footwall damage zone across the mylonite along the Monapo River (westward from the village of Monapo, Fig. 2; Location D) indicates that the fabric is an L-S tectonite with intensity of the stretching lineations progressively increasing toward the mylonite. In the hanging wall, the shear fabric associated with the mylonite damage zone is obscured by the more complex earlier structural fabrics within the Metacheria Metamorphic Complex. Therefore, the shear fabric is only observed in isolation where rocks of the weakly deformed intrusive suites (Mazerapane and Ramiane) comprise the local hanging wall.

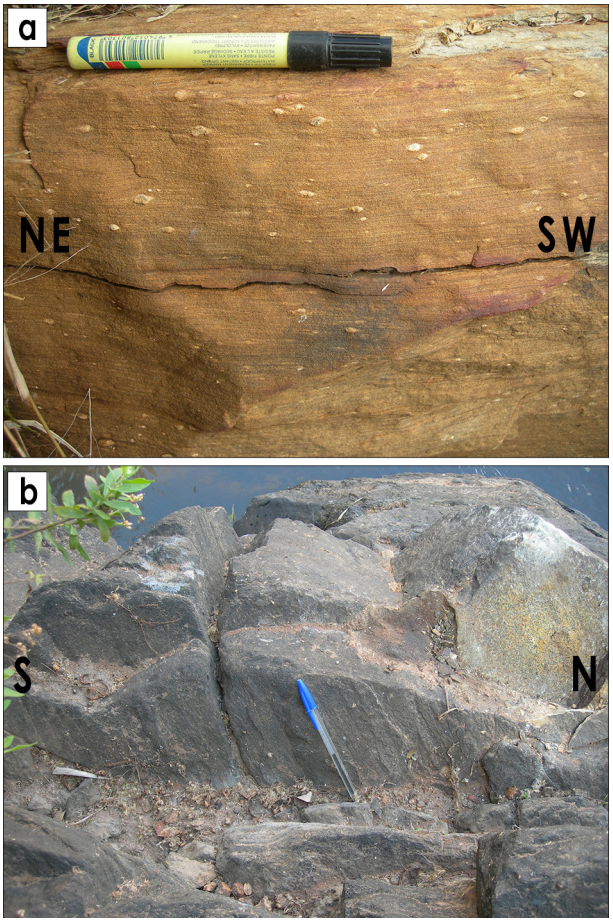

Fig. 3. (a) Quartz-rich mylonite containing feldspar clasts with subtly asymmetric tails. Rock face is parallel to mylonite zone and foliation is dipping in the view direction. (b) Intermediate amphibole-bearing marginal mylonite from Location B showing oblique stretching lineation on foliation surface.

4. Structural characterization

The Monapo Klippe and its footwall rocks have been divided into three structural domains based on their structural relationship to the klippe. These are the basement and footwall damage zone to the klippe, the klippe itself and the marginal mylonite that separates them. Fig. 4 shows a structural map of the Monapo Klippe, including measurements from these three structural domains.

4.1. Footwall damage zone

Footwall rocks outcrop prominently outside the Monapo Klippe on the northwest and southeast corners. There is little outcrop around the rest of the circumference and no observations could be made anywhere near the northeast margin of the klippe. Both areas show a strong pervasive foliation with an associated poorly developed, predominantly northeast plunging stretching lineation (Fig. 4a and b). The foliation data define two predominant orientations, one dipping steeply to the southeast and striking NE-SW (associated with outcrop in the northwest) and one dipping moderately to the west and striking N–S (associated with outcrop in the southeast). This is consistent with a broad asymmetric structural basin with its major axis trending approximately N–S, and also with the orientation of the overlying marginal mylonite, confirming the field relations reported by Macey et al. (2013).

4.2. Marginal mylonite

The orientation of the marginal mylonite was measured at only four locations (Fig. 2; Locations A, B, C, and D) around the klippe due to poor outcrop. It is important to note that since most of the foliation orientations were measured in the two outcrops on the west side of the klippe there is a strong bias in the contouring of the stereonet shown in Fig. 4c. Nevertheless, the moderately dipping foliation at the four locations of the marginal mylonite measured, which span a reasonable distribution about the klippe, indicate that the marginal mylonite everywhere dips into the klippe, consistent with an overall basinal structure. A strongly developed stretching lineation (Fig. 4d) observed as elongate ridges on the foliation surface is generally oriented down-dip, but in one location was oblique to the foliation. The orientations of lineations (Fig. 4d) are broadly similar to those measured in the footwall rocks (Fig. 4b).

4.3. Monapo Klippe

Structural measurements from within the Monapo Klippe are shown in Fig. 4e and f. The lineated planar fabric is termed S_2 after Macey et al. (2013). Lineation orientation is highly variable, and plunges predominantly either shallowly to steeply westward, or shallowly to steeply eastwards. S_2 is consistent within individual

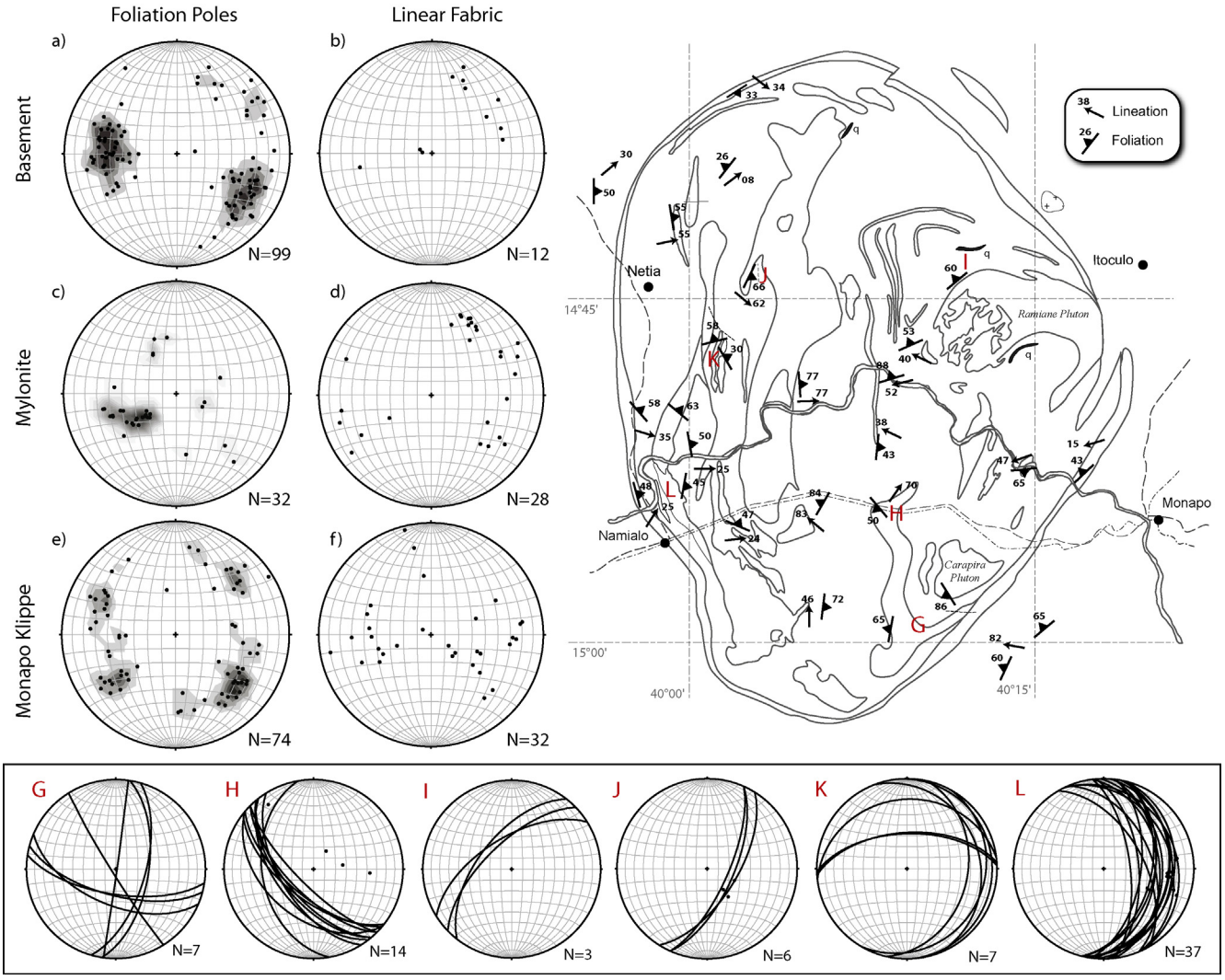

Fig. 4. (Left) Equal area, lower hemisphere stereonets showing all contoured foliation poles and linear fabric measurements for sites in the footwall surrounding the klippe (a and b), the marginal mylonite (c and d), and within the Monapo Klippe rocks (e and f). Foliation pole stereonets are contoured with 1% area contours with contour interval 2.0%/1% area. (Right) Structural map of the Monapo Klippe and surrounding footwall rocks, showing outlines of lithological units and structural measurements. (Bottom) Stereonets (G–L: corresponding to red letters on map) showing the spatial variation in fabric orientation (foliation planes and linear fabrics) within the Monapo Klippe.

outcrops (G–L; Fig. 4) but varies spatially around the klippe. The orientations are locally similar to S_2 in the footwall (dipping towards the east or northwest; Fig. 4a) but more broadly distributed, locally dipping also toward the southwest. Overall, this distribution is consistent with folds with wavelengths on the 100s–1000s meters-scale previously inferred from lithologic patterns by Macey et al. (2013). The similarity with footwall fabrics and the broad basin in the marginal mylonite is consistent with the idea that these smaller structures have been rotated in a common deformation event that formed the larger (10s km-scale) basinal shape of the klippe.

5. Shear sense

The rarity and deep weathering of the mylonite field outcrops made shear sense determination in the field difficult. Recrystallization of the mylonite has obscured grain-scale shear sense indicators in the matrix. The predominant scale of preserved shear sense indicators (mainly mm-scale clasts), favours shear sense determination in the marginal mylonite at hand-sample scale. However, extreme flattening, symmetry and rarity of clasts makes recognizing clast orientation and tail asymmetry to interpret shear direction problematic (Fig. 5a). Therefore, a combination of field observations and XCT imaging has been used to determine as accurately as possible the shear sense in samples from each of the studied outcrops.

5.1. Field based shear sense determination

At each of the four locations (A–D, Fig. 2), the orientations of the mylonitic foliation and stretching lineation were determined. Shear sense determination depended on the particular fabric at each outcrop. Where possible, the ductily sheared damage zone kinematic indicators were compared to those measured within the mylonite at each outcrop location.

5.1.1. Location A

At Location A on the northern margin of the klippe (Fig. 2) the outcrop is comprised of two different mylonitic rock types. The characteristic quartz-rich mylonite containing <1 cm almond-shaped tailed clasts of feldspar (Fig. 3a), and a structurally higher penetratively lineated amphibole-rich mylonite lacking clasts. The lineated amphibole-mylonite is very weakly foliated and the stretching lineation, defined by elongation of amphibole and feldspar grains, is parallel to the lineation as measured in the quartz-rich mylonites (plunge/trend = 36/133). In the quartz-rich

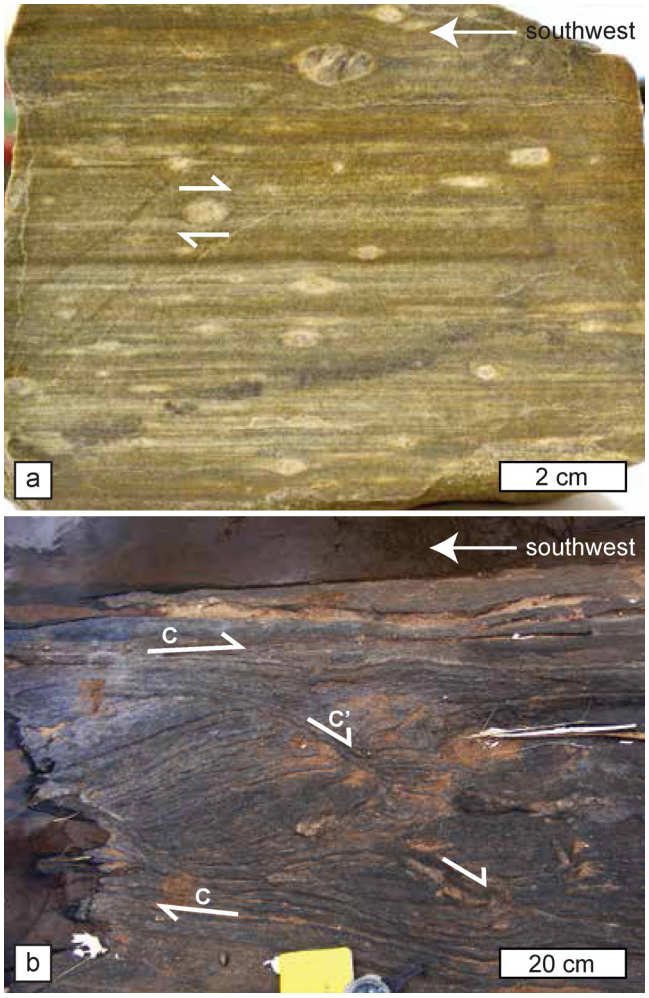

Fig. 5. Meso-scale shear sense determination in the marginal mylonite. (a) Slabbed slice through Sample JM06MC10 from Location A (Fig. 2) showing numerous clasts within a strong penetrative foliation. Shear sense indicators are shown with (σ) or (δ) indicating the type of tailed clast. Clasts with ambiguous or symmetric tails are indicated with (ϕ). (b) Field photo of Location D showing single occurrence of C–C′ fabric in foliated clast-free mylonite on Monapo River transect. Annotations show apparent shear on C and C′ fabric surfaces, respectively.

member, the lineation is expressed as sub-millimetre corrugations on the foliation surface. The rock cleaves readily along the foliation (strike/dip = 074/42 S) and the lineation is easily recognized throughout the outcrop.

Shear sense at Location A was established by careful examination of tailed clasts in outcrop exposure and analysis of oriented slabs in both the quartz-rich and amphibole-rich mylonites (n = 146 clasts). 40% of grains had identifiable asymmetric tails, of which 86% indicated normal motion (Fig. 5a). Locally the lineation in the footwall damage zone rocks roughly correlates to that measured at Location A where shear sense is established. In their current orientation, these kinematic indicators suggest normal motion, noting that the stretching lineation is oblique to the dip of the foliation. At this outcrop in the current geometry this indicates top to the SE transport.

5.1.2. Location B

On the western side of the Monapo Klippe, the mylonite is exposed at Location B (Fig. 2) where a tributary of the Monapo River passes under an old derelict road bridge. The outcrop is mostly below water during the wet season but is accessible on the edges of the riverbed during the dry season. Strike length of the outcrop is about 12 m along the riverbank. The mylonite at this location is compositionally heterogeneous and appears to be derived from the intermediate to mafic granulites of the Metacheria Metamorphic Complex. Sections perpendicular to the foliation indicate a pronounced banding defined by alternating layers of mafic and felsic material. A localized oblique foliation is developed that defines a S–C structure within the planar foliation (325/27 E). The stretching lineation (25/026) is oblique to the dip of the foliation. The rock contains both δ and σ clasts, principally of quartz and/or feldspar with δ clasts dominant. Overall, asymmetrical clasts are rare, however normal shear sense suggested by σ- and δ-clast orientations in slabbed samples is consistent with observed S–C fabrics at this location indicating top to the northeast transport.

5.1.3. Location C

South of Location B, the marginal mylonite is exposed at Location C where the Namialo-Netia road crosses a tributary just north of the Monapo River (Fig. 2). Like Location B, this outcrop is mostly below the water during the wet season and is only accessible during the dry season. Strike-length of the outcrop is ~20 m along the riverbank. The mylonite consists of a coarse-grained sugary matrix with a flaky planar foliation (349/49 E) containing tabular to boudin-shaped blocks of less intensely sheared rock. These blocks form elongated clasts <1 cm to 40 cm long whose asymmetry can be used to determine shear sense in the mylonite. The clasts (n = 37) occur in both σ- and δ-clast morphologies. Although the majority of clasts are symmetrical as at Location A, the asymmetric clasts are in excellent agreement with 94% of asymmetrical clasts suggesting normal motion. As at the other outcrops, a strong stretching lineation (34/033) is manifested as a corrugation of the foliation surface as well as stretching of rigid pegmatitic injections along fabric but again, the lineation is oblique to the planar shear fabric. The clasts of less-deformed rock are dominated by mafic granulite which is locally abundant in the Monapo Klippe hanging wall. The present of R-shears, that attenuate clast tails and contribute to clast asymmetry, suggests that clasts have been shaped by a combination of brittle and ductile processes. All indicators show approximately normal shear sense at this location with top to the northeast transport in the current orientation and geometry.

5.1.4. Location D

At Location D, the outcrop is in a side channel of the Monapo River (accessible only during the dry season) on the eastern side of the klippe (Fig. 2) where the mylonite is extremely fine-grained and apparently clast-free. The S_2 foliation is planar and parallel (202/21 W) throughout the outcrop except for a 40-cm thick band of C–C′ structure. The C′-surfaces are asymptotic to the dominant shear fabric. The estimated motion vector (lying within the C-surface 90° away from C–C′ intersection) correlates to the measured stretching lineation (08/240) on the pegmatites which lies in the planar foliation and suggests reverse motion in the current orientation. The stretching lineations are at a moderate angle to the dip of the C-plane.

Observations along the Monapo River transect through Outcrop D display a correlation between the footwall damage zone fabrics and those within the mylonite. From the bridge where the major E–W highway crosses the Monapo River, a 5.5 km transect was examined of the footwall damage zone to the mylonite, and then a further ~2 km into the Monapo Klippe into the sheared damage zone in hanging wall rocks of the Ramiane Suite. Ductile shear fabrics across the transect dip at ~40° so this transect represents ~3 km structural thickness across the sheared footwall damage zone. The base of the damage zone was not identified, so 3 km is taken as a minimum local thickness. At the down-section end of the transect, the mylonite-parallel shear fabric is gently wavy and anastomosing and corrugations of the foliation surfaces form a weak lineation. The

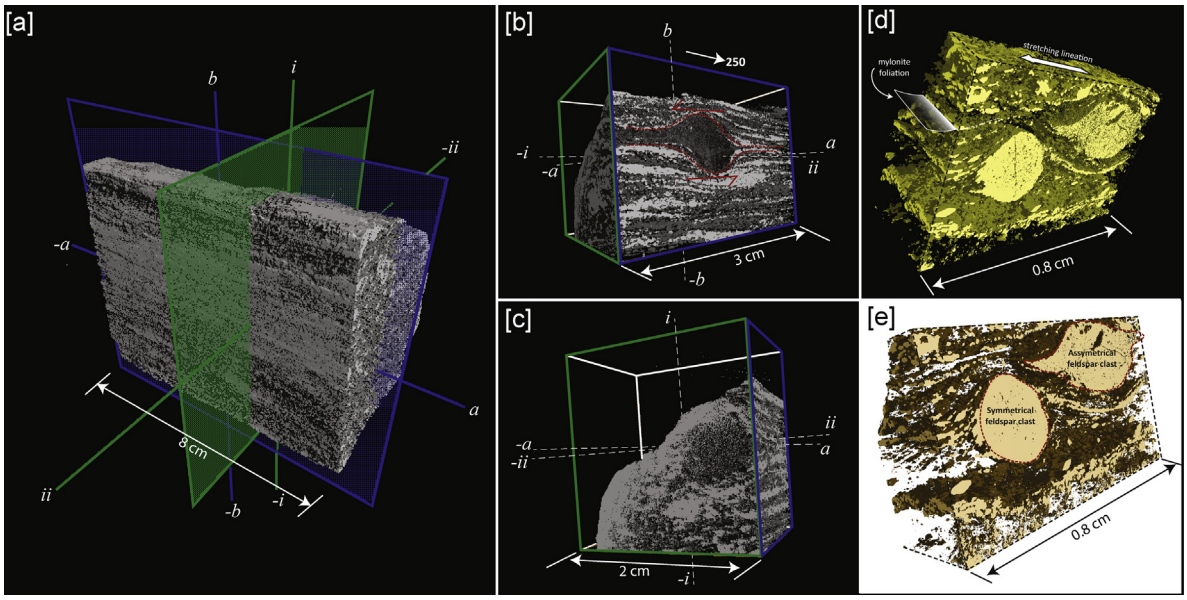

Fig. 6. Sectioning of mylonite samples via XCT. (a) 3D XCT image of whole sample with plane [*a*–*b*] parallel to the lineation; (b) 3D XCT image of same sample showing a sliced face in the [*a*–*b*] direction exposing a large δ-clast; (c) 3D XCT image of the same δ-clast as in (b) but along the face [i-ii] which is normal to that shown in (b). (d) 3D XCT image of symmetrical and assymetrical clasts within the mylonitic foliation with the low density fraction (quartz and feldspars) removed to highlight the 3D structure of the fabric. (e) 3D XCT image as shown in (d) but rotated to show the same clasts from a different orientation and with the black background replaced with a white background to illustrate the power of this technique for optimizing imaging of structural and mineralogical characteristics of rocks in 3D.

footwall gneisses along the transect belong to the Mamala Group of the Nampula Block and contain both biotite-rich and biotite-poor quartzo-feldspathic gneisses. This variation is observed throughout the transect and affects the local manifestation of folial and stretching fabrics which increase in intensity toward the mylonite.

5.1.5. Conditions of shearing

Locally in the uppermost footwall, trace amounts of syn-kinematic garnet have been identified in biotite-rich gneisses of the Molócuè Group. Garnet is rarely observed elsewhere in any lithologies of the Nampula Block and is therefore interpreted to have grown in response to deformation associated with the emplacement of the Monapo Klippe. In contrast, the shear fabrics in the highly localized mylonite, including the deformation of pegmatitic intrusions, include fractured feldspars. At Location C, in addition to syn-shearing pegmatitic intrusions as seen at other outcrops, thick tabular blocky quartz veins are found along foliation. The ends of the veins are pinched off along microfaults, suggesting minor attenuation of the veins. Aqueous fluid inclusions are prevalent although primary fluid inclusion assemblages could not be established. The veins are evidence for a late-stage fluid and microstructures in the quartz are consistent with deformation at greenschist-facies conditions.

5.2. XCT shear sense determination

A high proportion of clasts observed in outcrop showed no clast asymmetry (e.g. Fig. 5a), resulting in poor counting statistics. Therefore, outcrop-based shear sense determinations were confirmed with microstructural studies using XCT. XCT is a non-destructive method that produces a radial series of X-ray images through an object and computes a 3D tomographic image volume, which can then be sliced in any direction. The number of images taken can be determined by the operator based on the desired resolution of the final 3D reconstruction of the object. The 3D reconstruction displays differences in X-ray transparency (CT-number) with grayscale values (Fig. 6a), where the CT-number is a function of density, atomic number, and X-ray energy. Compositional differences between minerals are visible as different grayscale values. This technique has been shown to be extremely effective at highlighting anisotropies in rocks (Ketcham and Carlson, 2001; Ketcham, 2005), and has been predominantly used to examine, for example, porosity and permeability in petroleum host rocks (Akin and Kovscek, 2003), soil structure and the ability of soils to transport fluids (Heijs et al., 1995; Elliot et al., 2010), and to a lesser extent porphyroblast grain shape in metamorphic rocks (Ketcham et al., 2005; Huddleston-Holmes and Ketcham, 2010), and igneous rock textures (Baker et al., 2012). The ability of this technique to identify these types of anisotropies should also allow it to identify 3D fabric elements in structurally complex rocks.

One advantage provided by XCT imaging over serial sectioning is that once a 3D reconstruction of a sample is made, it is possible to extract both 2D and 3D images of any section of the object in any orientation or spacing, and interpolate across slices of any thickness (Fig. 6b and c). Different CT-number regions (corresponding to grains of a particular mineral phase) can be made transparent to reveal the shape of individual grains (Fig. 6d and e). This process allows for the identification and characterization of many fabrics or objects within a sample that are not easily detected by other imaging methods, and minimizes effects of sample inhomogeneity usually encountered with traditional methods such as serial sectioning. In cases like the marginal mylonite, where textural overprinting is a risk, this technique allows easy identification of the true long axes of clasts and tails in three dimensions to determine asymmetry within the shear fabric (Fig. 6d and e). For this study three samples of mylonite (Location C – JM09MC02, and Location D – JM08MC35, JM08MC21) were imaged using XCT (Fig. 7).

5.2.1. Methodology

Samples were imaged using a General Electric Phoenix V|Tome|X L240 X-ray micro-CT scanner in the Central Analytical Facility at the University of Stellenbosch, South Africa. Sample JM09MC02 was processed separately as an initial exploratory sample. For this sample two thousand individual X-ray images were acquired with an image acquisition time of 500 ms per image,

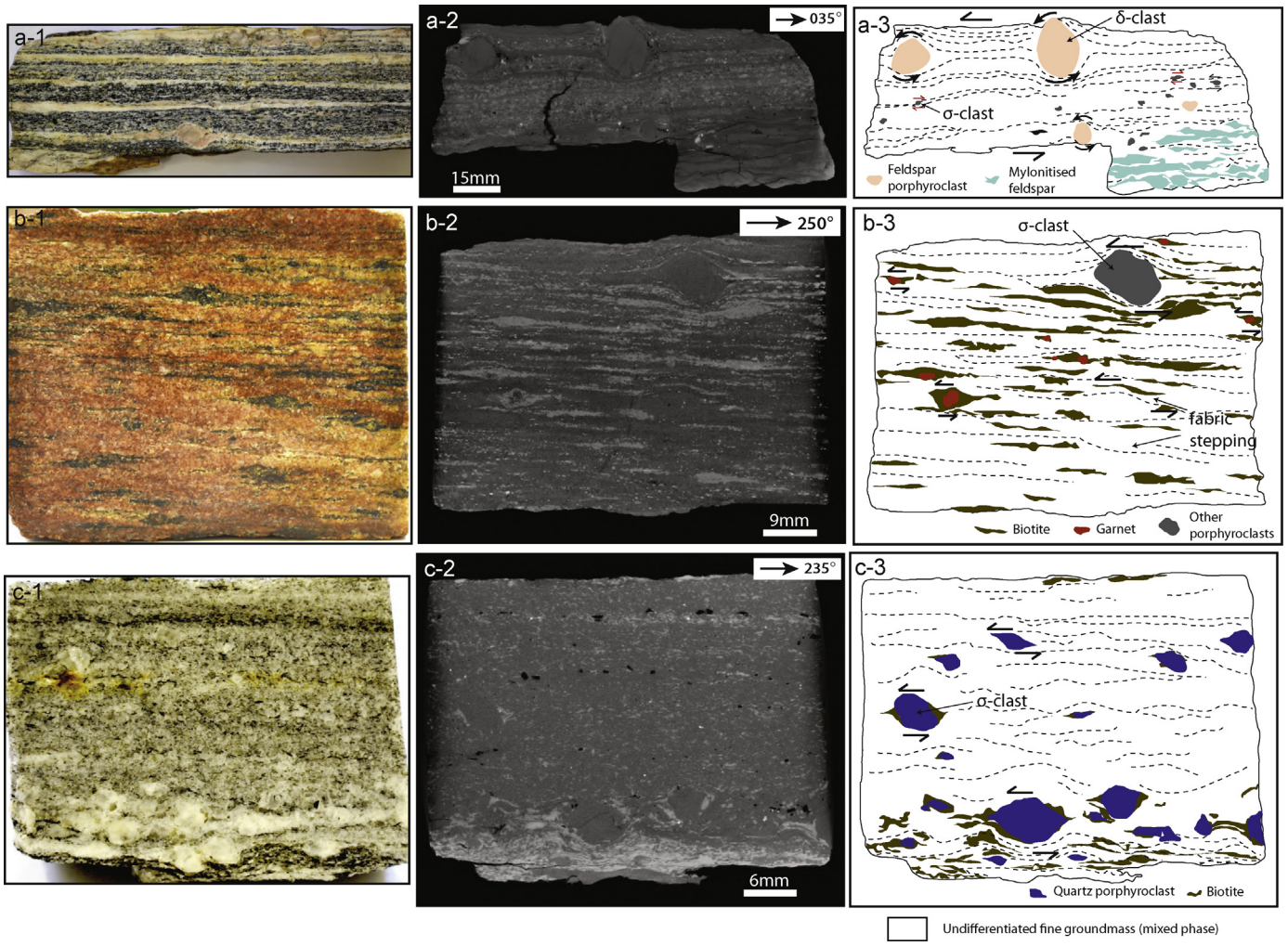

Fig. 7. Determination of XCT shear sense. Column 1 shows photographs of a polished external face on each sample cut parallel to the lineation and perpendicular to the shear foliation. Column 2 shows an XCT image for each sample taken from the stack of images. These images are X-ray images of a surface within each sample parallel to the surfaces photographed in column 1. Column 3 shows sketches of each XCT image, emphasizing foliation (dashed lines), porphyroclasts, and features that display shear sense. Sample a (JM09MC02): a-1 shows a layered rock with alternating dark and light bands and several feldspar porphyroclasts. In figure a-2 the porphyroclasts appear as a medium grey with light layers appearing as the darkest grey, and darker layers appearing as lighter-grey speckled layers. a-3 shows a sketch of a-2. Black grains represent distinctive grains within the matrix. Some show an opposite sense of shear to the larger grains, shown with arrows in red. Sample b (JM08MC35): b-1 shows an orange-brown rock with layers of black biotite. Occasional red-brown, round garnets are surrounded by biotite. In figure b-2 the biotite appears light grey, garnets very dark grey. b-3 shows a sketch of b-2 with a porphyroclast of undetermined mineralogy at the top of the sample showing a strong top-to-the east shear sense. Most smaller grains agree with this shear sense. Sample c (JM08MC21): c-1 shows a rock with asymmetric quartz clasts and a biotite fabric. c-2 shows biotite as light grey and quartz as dark grey. c-3 sketch shows biotite fabric, quartz porphyroclasts and biotite strain shadows.

averaging set to 2 (for every projection image, two images are taken and averaged to reduce noise), and with no skipping. Images were taken with a nanofocus NF180 tube with an accelerating voltage of 180 kV and a current of 140 μA. The total scan time was approximately 35 min and the voxel size for the 3D image produced is 85 μm. Samples JM08MC35, JM08MC21 were processed under the same conditions. For these samples 3000 images were acquired for each sample with an acquisition time of 1 s per image, without averaging or skipping of images. The nanofocus NF180 tube was again used with an accelerating voltage of 160 kV and a current of 160 μA. The total scan time for each sample was approximately 50 min. Typical voxel sizes for the 3D images produced were from 47 to 69 μm, depending on the samples physical size.

Volume reconstruction for all samples was done using the system-supplied Datos reconstruction software. The obtained 3D data set was analysed using Volume Graphics VGStudioMax 2.1. In this case only contrast enhancement was used to image features of interest. For optimal shear sense observation, each 3D volume was sliced into a series of 2D images spaced 85 μm apart in an orientation parallel to the sample's linear fabric (estimated from field observations and confirmed from long axis of clasts observed in the 3D volume) and normal to foliation. Shear sense was determined from these image stacks for each sample, using ImageJ 1.42q freeware. Image sequences were processed as a stack so that each sample could be viewed in its entirety as a video moving through the rock orthogonal to the image orientation. Porphyroclasts, here defined as clasts larger than the average grain size of each samples' matrix, were counted and, where distinguishable, shear sense was determined.

Sheared porphyroclasts were classified using the system described by Passchier and Trouw (2005, Chapter 5.6) for classification of porphyroclasts in mylonite. In the three samples most shear sense indicators occurred as: (1) mantled porphyroclasts with asymmetric tails (winged clasts); (2) mantled porphyroclasts with recrystallized minerals in the strain shadow; (3) sigmoid clasts; or (4) mineral fish. All porphyroclasts were classified as having either δ, σ, or ϕ morphologies, or as mineral fish for ease of classification, and because porphyroclast mantles and cores often

Table 1
Shear sense counting statistics determined from computer tomography images.

Sample	Total grains counted (*N*)	Clast type				Shear sense (vergence) inferred from clast tail asymmetry of δ and σ clasts and mineral fish				
		δ	σ	ϕ	Mineral fish	NE	E	W	SW	Symmetric
JM09MC02 (Fig. 7a)	51	22 (43%)	16 (31%)	13 (25%)	0	33 (65%)	0 (0%)	0 (0%)	5 (10%)	13 (25%)
Average grain size	4.7 mm	4.8 mm	4.8 mm	4.4 mm	–	4.8 mm	–	–	4.64 mm	4.4 mm
JM08MC35 (Fig. 7b)	94	11 (12%)	46 (49%)	21 (22%)	16 (17%)	0 (0%)	61 (65%)	12 (13%)	0 (0%)	21 (22%)
Average grain size	3.6 mm	2.5 mm	3.5 mm	2.7 mm	4.7 mm	–	3.7 mm	2.9 mm	–	2.7 mm
JM08MC21 (Fig. 7c)	95	10 (11%)	77 (81%)	7 (7%)	1 (1%)	56 (59%)	0 (0%)	0 (0%)	32 (34%)	7 (7%)
Average grain size	2.4 mm	2.7 mm	2.3 mm	2.3 mm	2.1 mm	2.4 mm	–	–	2.2 mm	2.3 mm

had the same composition (and thus the same grayscale in XCT), and were therefore difficult to distinguish. The grain types and dominant shear sense is shown in Table 1 and Fig. 7. Total grains counted (*N*) refers to the total number of observable porphyroclasts in the sample. All grain sizes described were measured parallel to the long axis of the grain.

5.2.2. Sample JM09MC02

This sample of mylonite from Location B (Fig. 2) is composed of fine-grained, banded felsic and mafic material (Fig. 7a). Within this sample, most clasts are located within the felsic bands. The clasts are 2–12 mm in size with an average grain size of 4.7 mm (Table 1). A total of 51 individual clasts could be identified. The majority of clasts are composed of round to oval-shaped feldspar porphyroclasts with tails of fine-grained feldspar and quartz. Forty-three percent of the counted clasts show δ geometry, 31% show σ geometry, and 25% show ϕ geometry (Table 1). The average grain size for δ and σ is slightly greater than for other porphyroclasts, however the difference is not large enough to be significant. Of the 51 clasts, 65% indicate overall top-to-the northeast shear sense and 25% exhibit no rotation (ϕ geometries) (Table 1). Clasts with top-to-the northeast shear sense also have a larger average grain size than clasts showing top-to the southwest shear sense. Because of this grain size difference, and since only 10% of the clasts indicate top-to-the-southwest shear sense, we conclude that at this location top-to-the northeast shear sense, is dominant.

5.2.3. Sample JM08MC35

This sample is mylonitized Ramiane Suite granite from Location D on the opposite side of the klippe to the previous sample (Fig. 2). It is composed of a banded fine-grained felsic matrix with 0.1–3 mm, round garnets surrounded by biotite mantles (Fig. 7b). A total of 94 1.5–11.5-mm-sized porphyroclasts were counted, with 12% of the clasts showing δ morphology, 49% showing σ morphology and 22% showing ϕ geometry (Table 1). The σ-clasts show a significantly larger average grain size than the δ and ϕ. In addition, there are a number of biotite sigmoid clasts (identified in hand specimen) and rare mineral fish. Since the XCT images only show compositional variation, individual mineral grains within sigmoids are not distinguishable, and therefore these clasts are difficult to distinguish from the mineral fish. Due to this, and for ease of comparison, we classified them as mineral fish. The biotite fish made up 17% of the total clasts counted, and show a significantly larger grain size than the other porphyroclasts. All the biotite fish, and the majority of the δ, and σ clasts (65% of total clasts counted) indicated top-to-the-east shear sense (Table 1). Clasts with top-to-the-east shear sense also have a significantly larger grain size than those with top-to-the-west shear sense. Since 22% of clasts showed no rotation, we conclude that this location has also been affected mainly by non-coaxial deformation with top-to-the-east sense of shear, and with a small component of coaxial deformation.

5.2.4. Sample JM08MC21

This sample is from the same location as JM08MC35 but has a stronger mylonite fabric. The sample is composed of fine-grained felsic material, with 1–5 mm quartz porphyroclasts, and exhibits less banding than other samples, with minor mafic layers (Fig. 7c). A total of 95 porphyroclasts were counted within the sample. The porphyroclasts occur as rounded δ- or σ-clasts with cores of quartz and mantles of fine-grained felsic material, quartz clasts with biotite strain shadows (here classified as σ-clasts), or biotite mineral fish. σ-Clasts are strongly dominant within the sample composing 81% of all porphyroclasts counted, with δ-clasts making up 11%, ϕ-clasts composing 7%, and mineral fish only 1% (Table 1). There is very little difference in the average grain size of the different porphyroclast morphologies, with the dominant top-to-the-northeast shear sense indicators showing a slightly larger average grain size than the less numerous top-to-the-southwest clasts. We therefore conclude that deformation at this location was predominantly non-coaxial with a top-to-the-northeast shear sense. However in comparison to other mylonite samples, the higher relative proportion of clasts with an opposite shear sense suggests that this sample may preserve evidence of more complex strain history than the other samples.

5.2.5. Summary

The microstructural shear sense indicators observed in XCT images are generally similar, indicating top-to-the-east to northeast shearing, consistent with the field observations. The orientation of the shear planes in which the shear sense was measured varies from place to place consistent with the overall basinal shape of the marginal mylonite.

6. Discussion

The shear sense, relative timing indicators, and constraints on conditions of activity allow us to compare the evidence for shearing on the Monapo mylonite with regional models proposed by other workers based on geochemistry (Grantham et al., 2008, 2013), geochronology (Bingen et al., 2009; Ueda et al., 2012a,b; Emmel et al., 2011) and regional kinematics (Viola et al., 2008).

6.1. Geometry of the klippe and transport direction

The klippe is today characterized by a bowl shaped geometry (Fig. 4) with concentric curvilinear lithologic boundaries within the klippe (as seen in the northeast and southeast of the klippe, Fig. 2). Steeper foliation dips within the klippe in comparison to those seen on the marginal mylonite also indicate smaller map scale folds within the Monapo Klippe. The folding within the klippe is associated with higher temperature deformation and contained by the smooth contact of the marginal mylonite (Macey et al., 2013; this study). They are therefore interpreted to pre-date the development of the mylonite and the emplacement of the Monapo Klippe. Macey et al. (2013) suggested that the steeply dipping

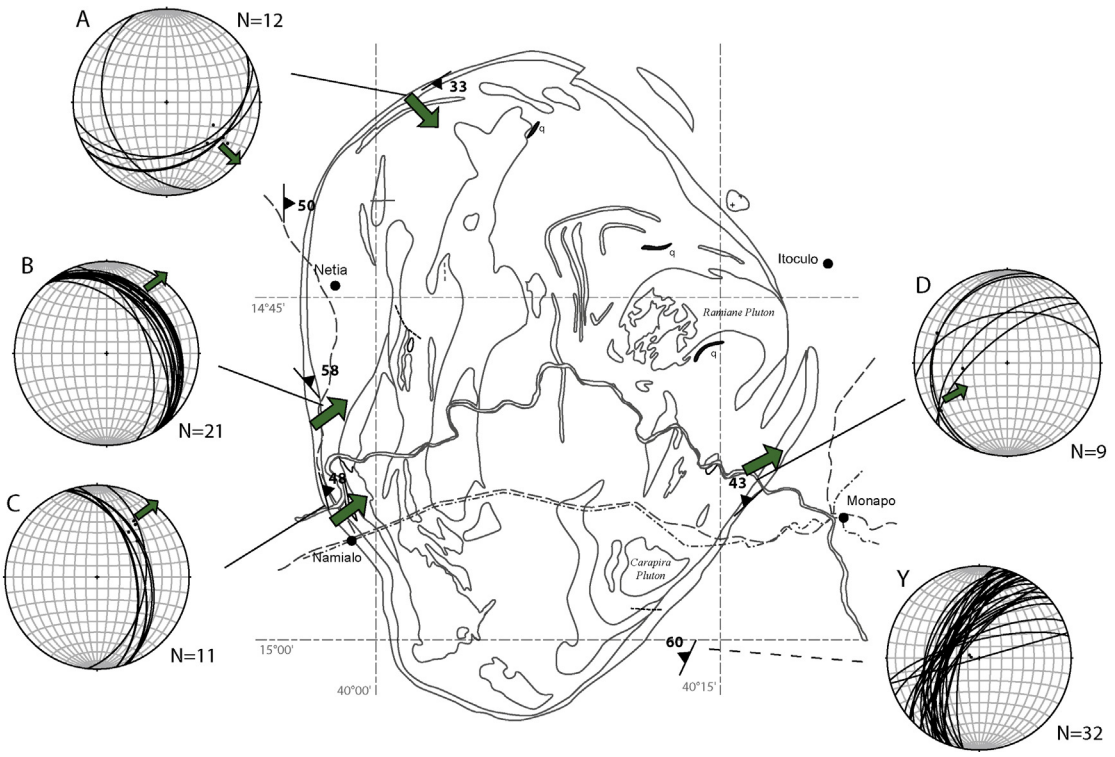

Fig. 8. Map of the Monapo Klippe with stereonets showing the spatial geometry (foliation planes) and linear fabrics of the mylonite (A–D) and footwall rocks (Y).

fabrics on the east and west side of the klippe indicate a regional synclinorium with a doubly plunging N–S trending axis. This is consistent with north–south trending folds of the same scale identified by Grantham et al. (2007, 2008) in the Nampula Block. The presence of shear sense indicators which show a down-dip, eastward sense of shear on the west side of the complex, and up-dip, eastward sense of shear on the eastern side of the complex indicates that the mylonite was folded subsequent to shearing. The moderate dips of the mylonite around the klippe reflect this post-emplacement folding event. Similar doubly plunging interference folds were described on regional to outcrop scales by Viola et al. (2008) in the Cabo Delgado Nappe Complex to the north as well as by Ueda et al. (2012a) for the northern Nampula Block.

The post-emplacement folding of the klippe has a bearing on the original transport direction of the klippe. The shape and scale of the basinal fold in which the klippe is currently preserved, is poorly constrained because of a lack of outcrop. Contouring of the combined foliation data shows four preferred orientations, which may reflect folding of the foliation, and show symmetry around N–S and E–W horizontal axes. Grantham et al. (2008, 2013) interpreted these as interference folds, formed during simultaneous N–S and E–W shortening. If this model is correct, shortening might be estimated from the fold scale and geometry. However, Ueda et al. (2012a,b) and Jacobs et al. (2008) favour megamullion-type deformation in an extensional environment as the mechanism of fold formation and in this case, interpreting foliation rotation around inferred fold hinges would not give a valid shortening estimate. The transport vectors in the mylonite (Fig. 8) all indicate northeasterly transport in the southern part of the klippe, and one vector measured in the north indicates southeasterly transport. Unfolding the klippe architecture might allow resolution of this scatter but, there is not sufficient information available to constrain the mode of formation of the long-wavelength folds. However, to rotate any of the transport vectors to a direction other than generally east, irrespective of the mechanism of post-emplacement folding, unrealistically large amounts of rotation on one or other set of vectors are required. Therefore, whilst we cannot precisely constrain the post-emplacement rotation, our data are only consistent with an easterly (northeast to southeast) transport direction during the last phase of motion on the Monapo mylonite.

6.2. Timing of transport of the Monapo Klippe

The geochronology of northern Mozambique is summarized in Fig. 9 and shown in comparison to the main orogenies that are thought to affect this region, specifically the East African Orogeny and the Kuunga/Malagasy Orogenies. The timing of transport of the Monapo Klippe must fit within the geochronological framework for northern Mozambique. However, tying the development of the Monapo mylonite to a specific period of time has been difficult because of the lack of datable material within the mylonite. Pegmatitic granite dykes are found both cross-cutting, and deformed by, the Monapo mylonite. At Locations B and C, intra-folial pegmatitic dykes occur within the mylonite and footwall damage zone and are sheared and stretched within the L–S fabric. These dykes are disaggregated in elongate boudins parallel to local stretching lineation with larger (2–5 cm) feldspar crystals forming rigid augen (Fig. 10a). At Location B, highly attenuated pegmatitic dykes lie in the foliation plane, whilst undeformed tabular pegmatitic dykes also crosscut the mylonitic foliation at a high angle. Structurally upsection from the mylonite, a large pegmatitic granite intrusion contains xenoliths of mylonite up to 30 m long by 3 m wide (Fig. 10b). These mutual crosscutting relationships require that these intrusions were contemporaneous with deformation of the Monapo mylonite. Unfortunately efforts to date these pegmatites have been unsuccessful with zircons from both rock types being undatable because of their extremely metamict state.

Granitic intrusions of Late Neoproterozoic to Ordovician age are common in the Nampula Block and less common in the Namuno Block (Viola et al., 2008; Bingen et al., 2009; Thomas et al., 2010; Macey et al., 2010, 2013). Two main groups are distinguished: (1) Late Neoproterozoic granites of the Monte Maco and Miruei Suites

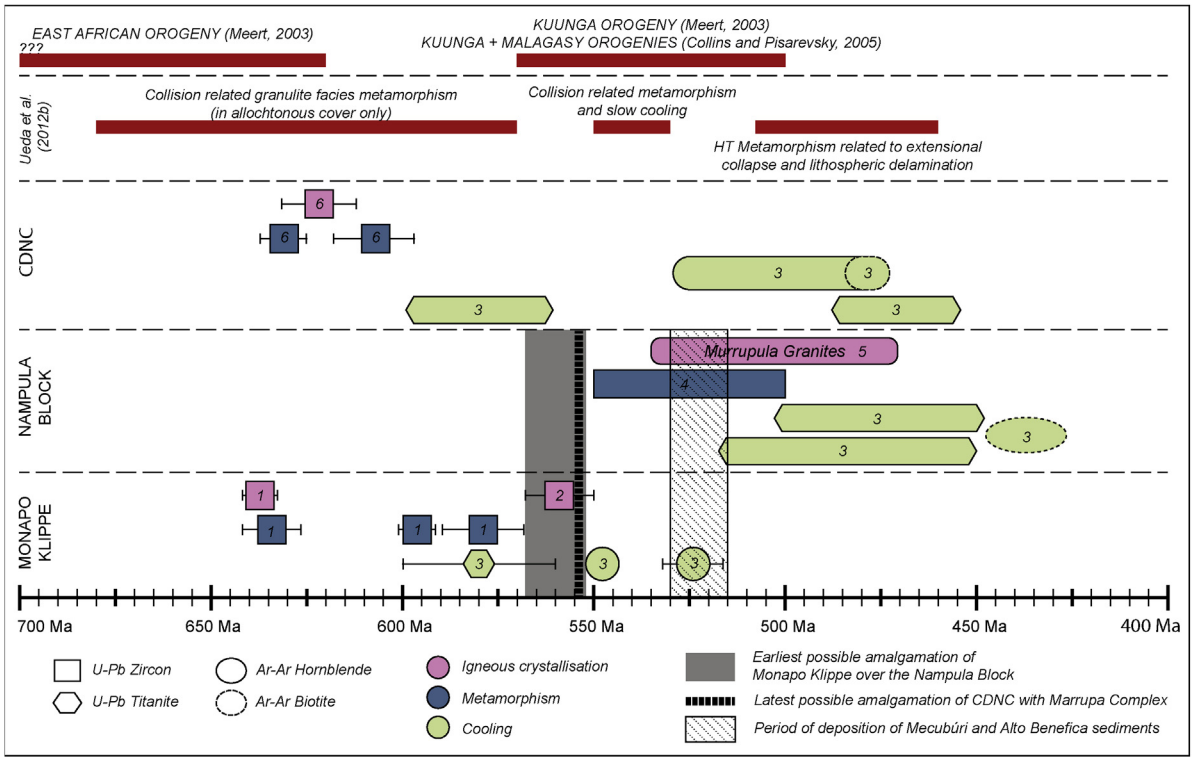

Fig. 9. Summary of geochronology from the Monapo Klippe, Nampula Block, Cabo Delgado Nappe Complex (CDNC) and Marrupa and Unango complexes and comparison to the timing of major events as outlined by Meert (2003), Collins and Pisarevsky (2005) and Ueda et al. (2012b): [1] Macey et al. (2013); [2] Jamal (2005); [3] Ueda et al. (2012b); [4] Macey et al. (2010); [5] Bingen et al. (2009), Macey et al. (2010); [6] Boyd et al. (2010).

with ages of ~575–545 Ma and which occur to the north of the Lúrio Belt; and (2) voluminous Cambrian to Ordovician granites which include the Murrupula, Niassa and Malema suites, with ages between ~535 and 470 Ma which occur both north and south of the Lúrio Belt (Figs. 1 and 9) (Grantham et al., 2007). All the granites south of the Lúrio Belt are attributed to the Murrupula Suite, which encompasses pegmatitic to aplitic granites that are generally undeformed (Macey et al., 2007; Grantham et al., 2007). Jamal (2005) and Ueda et al. (2012a) documented both deformed and undeformed granites in the Lúrio Belt and Nampula Block with magmatic ages of ~515–500 Ma. Undeformed Murrupula porphyritic granitoids dated by Macey et al. (2007) and Grantham et al. (2007) give crystallization ages from 533 to 497 Ma. It has been suggested that these granites are either post-collisional intrusions associated with orogenic collapse of a hypothesized East African Antarctic Orogen (Jacobs et al., 2008; Thomas et al., 2010; Ueda et al., 2012a,b) or that they have formed from melting as a result of crustal thickening during continental convergence (Grantham et al., 2013).

The key to the timing of emplacement of the klippe based on the cross-cutting pegmatites therefore comes down to whether the pegmatites are part of the Ramiane Suite, in which case they are likely to be Neoproterozoic in age, or whether they are part of the Murrupula Suite, in which case they are likely to be Cambrian to Ordovician in age. Resolving this issue is key to linking emplacement with an older orogenic event (the East African Orogeny) or a younger orogenic event (possibly the postulated Kuunga or Malagasy orogenies: Meert, 2003; Collins and Pisarevsky, 2005; Fritz et al., 2013). True Murrupula Granites are found in close proximity to the Monapo Klippe. The Monts de Nampaco pluton is approximately 10 km to the south of the klippe whilst the Ceia pluton is approximately 10 km to the south west of the klippe. These two plutons have been dated at 521 ± 4 Ma and 514 ± 4 Ma respectively by SHRIMP U–Pb dating (Fig. 9) (Grantham et al., 2007). In addition, both of these plutons are porphyritic with medium to large feldspar phenocrysts similar to the pegmatites cross-cutting the marginal mylonite. Moreover, the Ramiane Suite granites preserve evidence for a younger, relatively high-grade metamorphic overprint at ~596 Ma (Macey et al., 2013). This indicates their emplacement must have significantly predated the emplacement of the klippe as the undeformed pegmatites are cross-cutting a mylonite that continued to develop and evolve into upper greenschist-facies conditions. Finally, there do not appear to be any Murrupula Suite granites intruding into the klippe itself, which suggests that it was not emplaced into its current location until after the granites had been emplaced, or that the marginal mylonite represented a rheologic barrier to intrusion. In combination, all these points strongly indicate that the pegmatites cross-cutting the marginal mylonite are related to Murrupula Suite granites and therefore the emplacement of the klippe occurred during Cambrian to Ordovician times in the interval ~530–490 Ma. This is consistent with the regional extension and exhumation beginning at ~530 Ma and high-temperature low-pressure metamorphism at ~515–460 Ma associated with migmatization and granite magmatism south of the Lúrio Belt (Fig. 9) (Ueda et al., 2012b).

6.3. Implications for regional models

The discrete mylonites which underlie the Monapo Klippe consistently record dominantly east–west stretching lineations and kinematic indicators show eastward transport. If this granulite klippe is an equivalent of the extensive granulite terranes to the north, specifically the Cabo Delgado Nappe Complex as previous work suggests, it would need to have been emplaced by southwestward thrusting at high temperatures during the late Neoproterozoic. As no south-vergent kinematics were observed in this study, there is no evidence to support the interpretation that the klippe was originally rooted in the north and transported to the south. This model has been presented by Grantham et al. (2013)

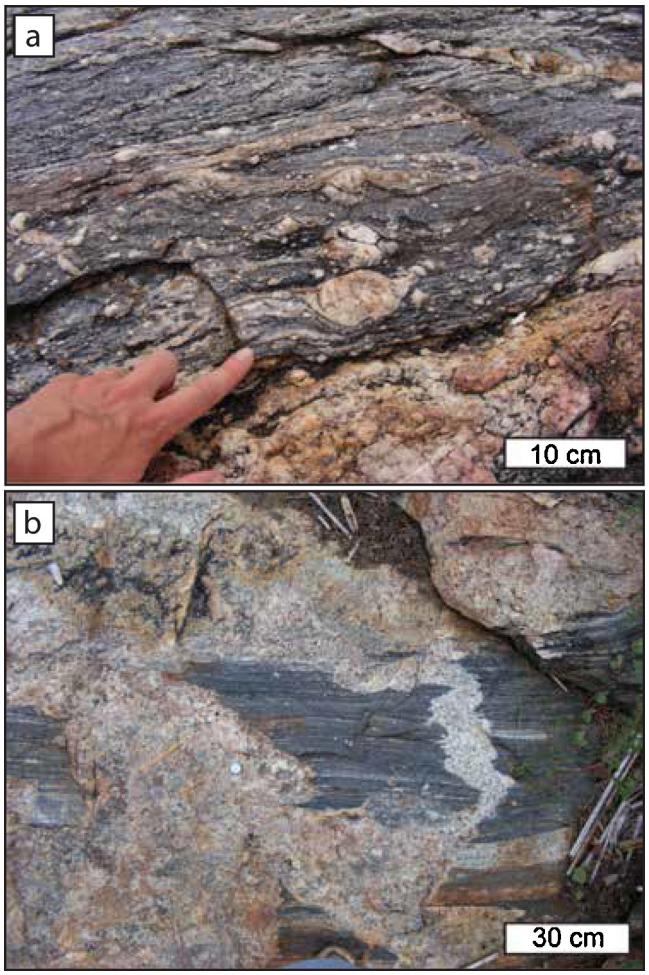

Fig. 10. Mutual crosscutting between Monapo mylonite and pegmatitic granite intrusions. (a) Potassium-feldspar augen formed by deformation of pegmatitic granites due to shearing of ductile foowall damage zone a few metres downsection from Location B. (b) Xenoliths of Monapo mylonite within large pegmatitic granite body a few metres upsection from Location B.

and Macey et al. (2013), where they have suggested that the Monapo Klippe was part of a mega-nappe sheet that was thrust south over a large part of central Gondwana, extending to Dronning Maud Land in Antarctica. The Viola et al. (2008) and Ueda et al. (2012a,b) model for assembly of northern Mozambique requires that the Monapo Klippe, as part of the Cabo Delgado Nappe Complex, was originally emplaced by north westward thrusting of a large nappe sheet over both the Namuno and Nampula blocks. The east-vergent kinematic indicators observed in this study could therefore reflect reactivation of the emplacement surface during regional east–west directed extension between ~520 and 440 Ma. However, it should also be noted that west-vergent kinematics were also not observed in this study and so we can also not provide any concrete evidence in support of original westward thrusting of the Cabo Delgado Nappe Complex over both the Namuno and Nampula blocks. Indeed, from the timing evidence presented above it seems unlikely that the emplacement of the Monapo Klippe was related to west-vergent kinematics in the Namuno Block identified by Viola et al. (2008) as these seem to part of an earlier history (Fig. 11) and probably related to the development of the East African Orogen.

Ueda et al. (2012b) show significant differences in the timing and rate of exhumation between the terranes north and south of the Lúrio Belt. The protracted high-temperature, low pressure metamorphism and anatexis in the Nampula Province is dated at 515–460 Ma (Fig. 9), but Ueda et al. (2012b) do not report structural observations supporting regional extension. The mutually cross-cutting relationships between the Monapo mylonite and the undated pegmatites (Fig. 10) are consistent with the inference that the final eastward transport of the Monapo Klippe may be related to this event. Ueda et al. (2012b) and Emmel et al. (2011) report a long cooling period with temperatures (of rocks currently exposed at the surface) held above 600 °C until at least 470 Ma. Emmel et al. (2011) suggest that the difference in crustal level exposed north and south of the Lúrio Belt might be as much as 10 km or more, with low and homogenous exhumation rates related to isostasy and erosion dominated uplift since the Mesozoic.

Our results would support the tectonic models from geochronology which infer post-orogenic delamination of the lower plate south of the Lúrio Belt (e.g. Ueda et al., 2012a,b). Although the origins of the Lúrio Belt are still being debated, it does appear to mark a clear division between areas to the north which are exposed at a higher structural level, preserving the granulite nappe complexes, and areas to the south which are exposed at or below the base of the granulite nappes, and are thought to have experienced delamination-associated heating starting at ~520 Ma (Fig. 9). The wide zone of ductile fabrics in the hanging wall and footwall of the Monapo mylonite may date from the original emplacement of the nappes, and is crosscut and overprinted by eastward reactivation along a discrete mylonite zone during exhumation. The inferred prolonged period of high temperatures in the region (Emmel et al., 2011; Ueda et al., 2012b) could therefore explain the annealing of the quartzo-feldspathic matrix of the Monapo mylonite.

The transport direction determined in this study adds to a very limited data set of kinematics indicators associated with Gondwana assembly. Fig. 11 shows this diagrammatically in the context of Cambrian Gondwana. Eastward transport vectors have been established in Madagascar by Collins et al. (2003), and in Sri Lanka by Kriegsman (1995) whereas northwest transport has been established in northern Mozambique by Viola et al. (2008). However, these vectors indicate transport at different times. Eastward transport in Madagascar is considered to have occurred between 530 and 515 Ma (Collins et al., 2003), that in Sri Lanka is constrained to ~580 Ma (Kriegsman, 1995), whilst westward transport north of the Lúrio Belt is thought to occur between 630 Ma and 590 Ma. This older phase of westward thrusting is consistent with observations in Tanzania to the north (e.g. Thomas et al., 2012).

Although there has been a considerable amount of debate within the literature regarding Neoproterozoic to early Palaeozoic orogenic events such as the Kuunga Orogeny, the East African Orogeny or the East African-Antarctic Orogeny, and the ubiquitous Pan-African Orogeny, there continues to be a lack of clarity over what each orogen represents, which metamorphic belts were affected and the relationship spatially separated orogenic belts of the same age. This is perhaps most clearly evident in use of the term Pan-African Orogeny, which a scan of current literature would suggest occurs over such an immense area of Gondwana and over such a protracted period of time that it cannot in reality be a single orogenic event. In the context of the Monapo Klippe in northern Mozambique, recent studies have suggested that the emplacement of the Monapo Klippe is the result of the post-orogenic collapse (Macey et al., 2013). Viola et al. (2008) and Ueda et al. (2012a,b) imply that this would be collapse of an East-African-Antarctic Orogen as opposed to an East-African Orogen. However, this would link the Monapo Klippe into an immensely long orogenic belt, stretching over 7500 km from southern Israel, Jordan and Sinai in the north to central Antarctica in the south. From the results of this study and from the compilation of geochronological data presented in Fig. 9 we think that this is unlikely. The East African Orogeny can best be ascribed to the mid-Neoproterozoic and is mostly associated with orogenic belts further north in Africa, apparently not extending further south than northern Mozambique and Madagascar (Fritz et al.,

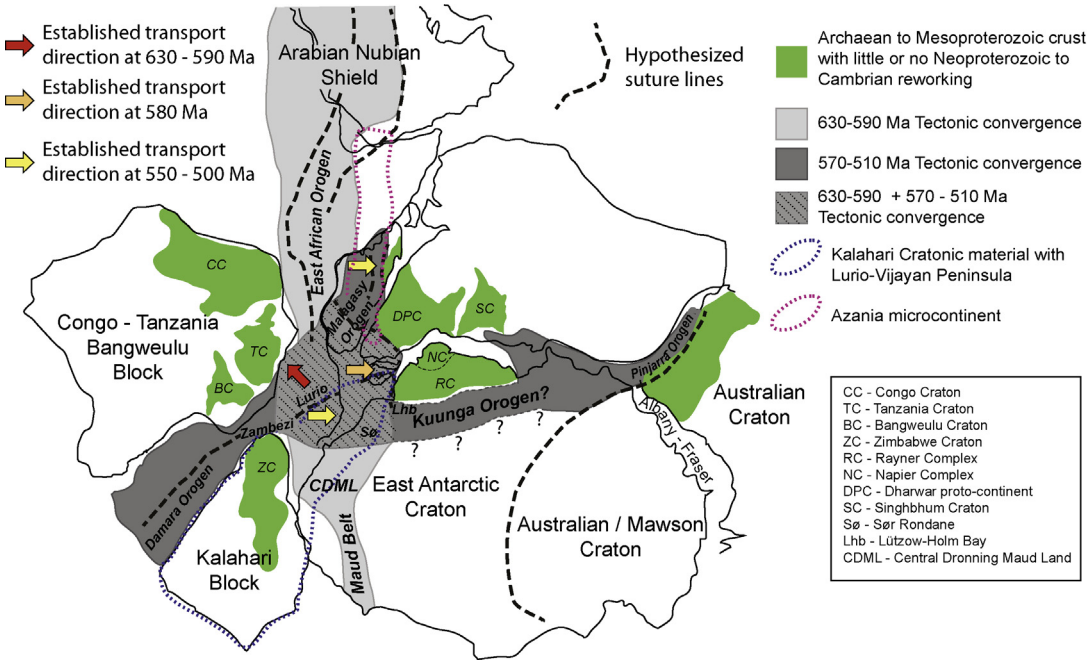

Fig. 11. Reconstruction of central eastern Gondwana during Late Neoproterozoic to Cambrian times. Redrawn from Meert (2003) with modifications from Collins and Pisarevsky (2005), Singh et al. (2010) and Collins et al. (2013). Transport directions from Collins et al. (2003), Viola et al. (2008), Collins et al. (2013), Kriegsman (1995) and this study.

2013). This orogeny appears to be characterized by west-directed vergence (e.g. Kriegsman, 1995; Thomas et al., 2012) and thus the north-west directed thrusting, probably linked to high-grade metamorphism in the Cabo Delgado Nappe Complex described by Viola et al. (2008) appears to be consistent with this event in both timing and kinematics (Fig. 9).

We agree that the current position of the Monapo Klippe is related to tectonic collapse of an orogen but suggest that this must be the result of a later and separate collisional phase that occurred after ~550 Ma (Figs. 9 and 11). The Monapo Klippe cannot have been emplaced over the Nampula Block until after ~570 at the earliest because the absence of the 590–570 Ma metamorphic event in the Nampula basement (Fig. 9). However, Bingen et al. (2009) have proposed that amalgamation of the Cabo Delgado Nappe Complex, which also experienced high-grade metamorphism in the time period ~630–610 Ma, must have been more or less completed by this time. We therefore suggest that the stacking of the Cabo Delgado Nappe Complex (of which the Monapo Klippe is a part) and the high grade metamorphism of this unit is a separate event to the stacking of the Monapo Klippe over the Nampula Block. The position of the Monapo Klippe south of its lithological- and metamorphic correlatives in the Cabo Delgado Nappe Complex has led previous workers to suggest that the Monapo and Mugeba klippen were emplaced by southward transport. This scenario has been postulated by Grantham et al. (2008, 2013) and Macey et al. (2013), who suggested that the metamorphism and deformation of the Mecubùri and Alto Benfica molasses sediments was in response to the over-riding of this large thrust sheet (Fig. 9). This study found no evidence for south-directed transport, but this does not exclude the possibility of an early phase south-directed transport. The Cambrian evolution of the Monapo Klippe appears to be consistent with wide-spread granite magmatism throughout central Gondwana. We therefore conclude that the eastward emplacement of the Monapo Klippe was part of a wide-spread post-orogenic collapse event during the terminal stages of Gondwana assembly resulting in crustal exhumation.

7. Conclusions

Kinematic indicators are extremely hard to find in the remnants of the crustal blocks that assembled into the supercontinent Gondwana. As such our understanding of Gondwana assembly is based for the most part on extensive geochronology databases and lithologic correlations. In many places this has given rise to conflicting interpretations of Gondwana assembly (e.g. Tucker et al., 2011 vs Collins et al., 2013). The Monapo Klippe represents a granulite-facies klippe thrust over the amphibolite-facies Nampula Block during the Neoproterozoic assembly of Gondwana. During transport from its original lower crustal position at peak metamorphism at ~635 Ma to emplacement in the middle or upper crust, the shear zone evolved from a diffuse ductile zone toward a narrow, lower-temperature high strain mylonite. This may have occurred during the northwest directed stacking of the Cabo Delgado Nappe Complex during the East African Orogeny at around 630–610 Ma. The Nampula Block developed a footwall damage zone of gradational L–S tectonite with local garnet possibly recording the metamorphic effect of over-thrusting by a hot nappe. Final motion was eastward along the thin marginal mylonite at mid-upper crustal conditions and is mutually cross-cutting with Cambrian to Ordovician granite intrusion and is therefore likely related to final late extension and collapse stages of Gondwana assembly.

Acknowledgements

This work was supported by the South African National Research Foundation on grant FA2007033000013 to C.D. Rowe and additional funding from Subcommittee B at Stellenbosch University to J.A. Miller. The stereonets shown in this manuscript were plotted using freely distributed Stereonet for Mac by Rick Allmendinger. Conversations with Giulio Viola helped clarify the complex history of regional models and greatly improved this manuscript. Taufeeq Dhansay, Meagan Webster, and Johann Diener are thanked for physical and mental field assistance during the 2008 field season. J.A. Miller thanks Alastair Beach for helpful discussion whilst

in the field. P.H. Macey publishes with the permission of the South African Council for Geosciences and acknowledges the field assistance of the Direcão Nacional Geologia Mozambique, particularly Carlos Fuma Camillo. We thank Joachim Jacobs, Giulio Viola and Kosuke Ueda for extremely helpful and thorough review of the manuscript.

References

Akin, S., Kovscek, A.R., 2003. Computed tomography in petroleum engineering research. Geological Society, London, Special Publications, vol. 215., pp. 23–28.

Baba, S., Hokada, T., Kaiden, H., Dunkley, D., Owada, M., Shiraishi, K., 2010. SHRIMP zircon U–Pb dating of sapphirine-bearing granulite and biotite-hornblende gneiss in the Schirmacher Hills, east Antarctica: implications for Neoproterozoic ultra-high temperature metamorphism predating assembly of Gondwana. Journal of Geology 118, 621–639.

Baker, D.R., Mancini, L., Polacci, M., Higgins, M.D., Gualda, G.A.R., Hill, R.J., Rivers, M.L., 2012. An introduction to the application of X-ray microtomography to the three-dimensional study of igneous rocks. Lithos 148, 262–276.

Bingen, B., Jacobs, J., Viola, G., Henderson, I.H.C., Skar, O., Boyd, R., Thomas, R.J., Solli, A., Key, R.M., Daudi, E.X.F., 2009. Geochronology of the Precambrian crust in the Mozambique Belt in NE Mozambique and implications for Gondwana assembly. Precambrian Research 170, 231–255.

Boyd, R., Nordgulen, O., Thomas, R.J., et al., 2010. The geology and geochemistry of the East African Orogen in northeastern Mozambique. South African Journal of Geology 113, 87–129.

BULGARGEOMIN (B.R.G.M.), 1984. Jazigo de apatite de Evate: resultos da pesquisa preliminary executada em 1981–1983, Maputo.

Collins, A.S., Clark, C., Plavsa, D., 2013. Peninsula India in Gondwana: the tectonothermal evolution of the southern granulite terrain and its Gondwanan counterparts. Gondwana Research, http://dx.doi.org/10.1016/j.gr.2013.01.002.

Collins, A.S., Fitzsimons, I.C.W., Hulscher, B., Razakamanana, T., 2003. Structure of the eastern margin of the East African Orogen in central Madagascar. Precambrian Research 123, 111–133.

Collins, A.S., Pisarevsky, S.A., 2005. Amalgamating eastern Gondwana: the evolution of the Circum Indian Orogens. Earth Science Reviews 71, 229–270.

Collins, A.S., Santosh, M., Braun, I., Clark, C., 2007. Age and sedimentary provenance of the Southern Granulites, South India: U–Th–Pb SHRIMP secondary ion mass spectrometry. Precambrian Research 155, 125–138.

Elliot, T.R., Reynolds, W.D., Heck, R.J., 2010. Use of existing pore models and X-ray computed tomography to predict saturated soil hydraulic conductivity. Geoderma 156, 133–142.

Emmel, B., Kumar, R., Ueda, K., Jacobs, J., Daszinnies, M.C., Thomas, R.J., Matola, R., 2011. Thermochronological history of an orogen-passive margin system: an example from northern Mozambique. Tectonics 30, TC2002, 21 p.

Fitzsimons, I.C.W., 2000. A review of tectonic elements in the East Antarctic Shield, and their implications for Gondwana and earlier supercontinents. Journal of African Earth Sciences 31, 3–23.

Fritz, H., Abdelsalam, M., Ali, K.A., Bingen, B., Collins, A.S., Fowler, A.R., Ghebreab, W., Hauzenberger, C.A., Johnson, P.R., Kusky, T.M., Macey, P., Muhongo, S., Stern, R.J., Viola, G., 2013. Orogen styles in the East African Orogen: a review of the Neoproterozoic to Cambrian tectonic evolution. Journal of African Earth Sciences 86, 65–106.

Grantham, G.H., Macey, P.H., Ingram, B.A., Roberts, M.P., Rohwer, M., Opperman, R., Manhica, V., Alvares, S., Bacalhau, Du Toit, M.C., Cronwright, M., Thomas, R.J., 2007. Map Explanation Sheets Meconte (1439) and Nacala (1440). National Directorate of Geology, Republic of Mozambique.

Grantham, G.H., Macey, P.H., Ingram, B.A., Roberts, M.P., Armstrong, R.A., Hokada, T., Shiraishi, K., Jackson, C., Bisnath, A., Manhica, V., 2008. Terrane correlation between Antarctica, Mozambique and Sri Lanka; comparisons of geochronology, lithology, structure and metamorphism and possible implications for the geology of southern Africa and Antarctica. In: Satish-Kumar, M., Motoyoshi, Y., Osani, Y., Hiroi, Y., Shiraishi, K. (Eds.), Geodynamic Evolution of East Antarctica: A Key to East–West Gondwana Connection. Geological Society, London, Special Publications, vol. 308, pp. 91–119.

Grantham, G.H., Macey, P.H., Horie, K., Kawakami, T., Ishikawa, M., Satish-Kumar, M., Tsuchiya, N., Graser, P., Azavedo, S., 2013. Comparison of the metamorphic history of the Monapo Complex, northern Mozambique and Balchenfjella and Austhameren areas Sør Rondane, Antarctica: implications for the Kuunga Orogeny and the amalgamation of East and West Gondwana. Precambrian Research.

Heijs, A.W., De Lange, J., Schoute, J.F.T., Bouma, J., 1995. Computed tomorgraphy as a tool for non-destructive analysis of flow patterns in macroporous clay soils. Geoderma 64, 183–196.

Huddleston-Holmes, C.R., Ketcham, R.A., 2010. An X-ray computed tomography study of inclusion trail orientations in multiple porphyrobalsts from a single sample. Tectonophysics 480, 305–320.

Jacobs, J., Fanning, C.M., Henjes-Kunst, F., Olesch, M., Paech, H.J., 1998. Continuation of the Mozambique Belt into East Antarctica: Grenville age metamorphism and polyphase Pan-African high grade events in central Dronning Maud Land. Journal of Geology 106, 385–406.

Jacobs, J., Bingen, B., Thomas, R.J., Bauer, W., Wingate, M., Feito, P., 2008. Early Palaeozoic orogenic collapse and voluminous late-tectonic magmatism in Dronning Maud Land and Mozambique: insights into the partially delaminated orogenic root of the East African-Antarctic Orogen? In: Satish-Kumar, M., Motoyoshi, Y., Osani, Y., Hiroi, Y., Shiraishi, K. (Eds.), Geodynamic Evolution of East Antarctica: A Key to East–West Gondwana Connection. Geological Society, London, Special Publications, vol. 308, pp. 69–90.

Jamal, D.L., 2005. Crustal studies across selected geotransects in NE Mozambique: differentiating between Mozambiquan (~Kibaran) and Pan-African Events, with implications for Gondwana studies. University of Cape Town, South Africa (unpublished PhD thesis).

Kelsey, D.E., Wade, B.P., Collins, A.S., Hand, M., Sealing, C.R., Netting, A., 2008. Discovery of a Neoproterozoic basin in the Prydz belt in East Antarctica and its implications for Gondwana assembly and ultrahigh temperature metamorphism. Precambrian Research 161, 355–388.

Ketcham, R.A., Carlson, W.D., 2001. Acquisition, optimization and interpretation of X-ray computed tomographic imagery: applications to the geosciences. Computers and Geosciences 27, 381–400.

Ketcham, R.A., 2005. Three-dimensional grain fabric measurements using high-resolution X-ray computed tomography. Journal of Structural Geology 27, 1217–1228.

Ketcham, R.A., Meth, C., Hirsch, D.M., Carlson, W.D., 2005. Improved methods for quantitative analysis of three-dimensional porphyroblastic textures. Geosphere 1, 42–59.

Kriegsman, L.M., 1995. The Pan-African event in East Antarctica: a view from Sri Lanka and the Mozambique Belt. Precambrian Research 75, 263–277.

Kröner, A., Sacchi, R., Jaeckel, P., Costa, M., 1997. Kibaran magmatism and Pan-African granulite metamorphism in northern Mozambique: single zircon ages and regional implications. Journal of African Earth Sciences 25, 467–484.

Macey, P.H., Ingram, B.A., Cronwright, M.S., Botha, G.A., Roberts, M.R., Grantham, G.H., Maree, L.P., Botha, P.M.W., Kota, M., Opperman, R., Haddon, I.G., Nolte, J.C., Rower, M., 2007. Map Explanation Sheets Alto Molócuè (1537), Murrupula (1538), Nampula (1539), Mogincual (1540), Errego (1637), Gilé (1638), and Angoche (1639–40). National Directorate of Geology, Republic of Mozambique.

Macey, P.H., Miller, J.A., Rowe, C.D., Grantham, G.H., Siegfried, P., Armstrong, R.A., Kemp, J., 2013. Geology of the Monapo Klippe, NE Mozambique and its significance for assembly of central Gondwana. Precambrian Research 233, 259–281.

Macey, P.H., Thomas, R.J., Grantham, G.H., et al., 2010. Mesoproterozoic geology of the Nampula Block, northern Mozambique: tracing fragments of Mesoproterozoic crust in the heart of Gondwana. Precambrian Research 182, 124–148.

Meert, J., 2003. A synopsis of events related to the assembly of eastern Gondwana. Tectonophysics 362, 1–40.

Norconsult Consortium, 2007a. Mineral Resources Management Capacity Building Project, Republic of Mozambique; Component 2: Geological infrastructure Development Project, Geological Mapping Lot 1; Sheet Explanation: 32 Sheets; Scale: 1/250000, Report No. B6.f. National Directorate of Geology, Republic of Mozambique.

Norconsult Consortium, 2007b. Mineral Resources Management Capacity Building Project, Republic of Mozambique; Component 2: Geological infrastructure Development Project, Geological Mapping Lot 1; Geophysical Interpretation, Report No. B4. National Directorate of Geology, Republic of Mozambique.

Passchier, C.W., Trouw, R.A.J., 2005. Microtectonics, 2nd ed. Springer Verlag, Berlin/Heidelberg/New York.

Pinna, P., 1995. On the dual nature of the Mozambique Belt, Mozambique to Kenya. Journal of African Earth Sciences 21, 477–480.

Pinna, P., Jourde, G., Calvez, J.Y., Mroz, J.P., Marques, J.M., 1993. The Mozambique Belt in northern Mozambique; Neoproterozoic (1100–850 Ma) crustal growth and tectogenesis, and superimposed Pan-African (800–550 Ma) tectonism. Precambrian Research 62, 1–59.

Sacchi, R., Cadoppi, P., Costa, M., 2000. Pan-African reactivation of the Lúrio segment of the Kibaran Belt system: a reappraisal from recent age determinations in northern Mozambique. Journal of African Earth Sciences 30, 629–639.

Satish-Kumar, M., Hokada, T., Owada, M., Osanai, Y., Shiraishi, K., 2013. Neoproterozoic orogens amalgamating East Gondwana: Did they cross each other? Precambrian Research 234, 1–7.

Shackelton, R.M., 1996. The final collision between East and West Gondwana: where is it? Journal of African Earth Sciences 23, 271–287.

Singh, Y.K., De Waele, B., Karmakard, S., Sarkara, S., Biswala, T.K., 2010. Tectonic setting of the Balaram-Kui-Surpagla-Kengora granulites of the South Delhi Terrane of the Aravalli Mobile Belt, NW India and its implication on correlation with the East African Orogen in the Gondwana assembly. Precambrian Research 183, 669–688.

Stern, R.J., 2004. Arc assembly and continental collision in the Neoproterozoic East African Orogen: implications for the consolidation of Gondwanaland. Annual Reviews in Earth and Planetary Sciences 22, 319–351.

Thomas, R.J., Jacobs, J., Horstwood, M.S.A., Ueda, K., Bingen, B., Matola, R., 2010. The Mecubùri and Alto Benfica Groups NE Mozambique: aids to unravelling ca. 1 and 0.5 Ga events in the East African Orogen. Precambrian Research 178, 72–90.

Thomas, R.J., Roberts, N.M.W., Jacobs, J., Bushi, A.M., Horstwood, M.S.A., 2012. Structural and geochronological constraints on the evolution of the eastern margin of the Tanzania Craton in the Mpwapwa area, central Tanzania. Precambrian Research 224, 671–689.

Tucker, R.D., Roig, J.Y., Macey, P.H., Delor, C., Amelin, Y., Armstrong, R.A., Rabarimanana, M.H., Ralison, A.V., 2011. A new geological framework for south-central Madagascar, and its relevance to the out-of-Africa hypothesis. Precambrian Research 185, 109–130.

Ueda, K., Jacobs, J., Thomas, R.J., Kosler, J., Jourdan, F., Matola, R., 2012a. Delamination-induced late-tectonic deformation and high-grade

metamorphism of the Proterozoic Nampula Complex, northern Mozambique. Precambrian Research 196-197, 275–294.
Ueda, K., Jacobs, J., Thomas, R.J., Kosler, J., Horstwood, M.S.A., Wartho, J.-A., Jourdan, F., Emmel, B., Matola, R., 2012b. Postcollisional high-grade metamorphism, Orogenic Collapse, and differential cooling of the East African Orogen of Northeast Mozambique. Journal of Geology 120, 507–530.
Viola, G., Hendersen, I.H.C., Bingen, B., Thomas, R.J., Smethurst, M.A., de Azavedo, S., 2008. Growth and collapse of a deeply eroded orogen: insights from structural and geochronological constraints on the Pan-African evolution of NE Mozambique. Tectonics 27, TC5009, http://dx.doi.org/10.1029/2008TC002284.